www.sciencemag.org/content/352/6293/1570/suppl/DC1

Supplementary Materials for

Reprogramming of avian neural crest axial identity and cell fate

Marcos Simoes-Costa and Marianne E. Bronner*

*Corresponding author. Email: mbronner@caltech.edu

Published 24 June 2016, *Science* **352**, 1570 (2016)
DOI: 10.1126/science.aaf2729

This PDF file includes:

Other Supplementary Material for this manuscript includes the following:
(available at www.sciencemag.org/content/352/6293/1570/suppl/DC1)

Database S1

Materials and Methods

Embryo electroporation

Fertilized eggs from white leghorn chickens were obtained from McIntyre Poultry & Fertile Eggs (Lakeside, California). Chicken embryos were electroporated *ex ovo* using previously described techniques (*14*). Briefly, embryos were dissected from the eggs using a filter paper ring and submersed in Ringer's buffer (*15*). Morpholinos or expression constructs were subsequently micro-injected in the space between the epiblast and vitelline membrane. Embryos were electroporated with platinum electrodes (five 50ms pulses of 5.1V, with an interval of 100ms between pulses). Following electroporation, embryos were cultured at 37^{o}C in sterile petri dishes containing fresh albumen until the desired stages. Embryo survival was >90%.

Embryo dissociation and cell sorting

After electroporation with 2ug/ul of the NC1:eGFP (cranial neural crest) or NC2:eGFP (trunk neural crest) enhancers, embryos were incubated at 37^{o}C until HH9+ and HH14 and screened for robust expression of GFP. Embryos with weak GFP expression or at incorrect stages of development were discarded. Dissected heads (HH9+) and trunks (HH14) were washed with dPBS and dissociated with Accumax (Accutase SCR006) cell dissociation solution. Reaction was stopped by addition of 10x the volume of Hanks solution supplemented with 0.5% BSA. Cells were subsequently washed, passed through a 40-µm cell strainer (BD Biosciences) and resuspended in Hanks 0.5% BSA. Efficiency of dissociation and cell viability was verified with trypan blue staining in a hemocytometer using an inverted tissue culture microscope. GFP+ cells were then sorted using a BD FACSARIA Cell Sorter (BD Biosciences) with 7-AAD exclusion to eliminate dead and damaged cells.

Library building and sequencing

Library building and sequencing was performed as previously described (*10*). Sorted cells were pelleted, washed with PBS and RNA was extracted with RNAqueous®-Micro Kit (Ambion AM1931). Quality of the RNA was assayed in an Agilent 2100 Bioanalyzer. All samples had RIN > 8. RNA was subsequently amplified with the Ovation RNA-Seq System V2 (NuGEN). The sequencing libraries were built according to the Illumina Standard Protocols. SR50 sequencing was performed in a HiSeq2000 Illumina machine. Sequence reads were aligned to the *Gallus gallus* genome with TopHat (*16*). Cufflinks and Cuffdiff (*17*) were used to calculate gene expression levels and identifying differentially expressed transcripts. Two cranial (stage HH9+, NC1:eGFP) and two trunk (stage HH14, NC2:eGFP) samples were processed together with Cuffdiff as replicates. A gene was considered to be expressed as part of the dataset if three conditions were met: (1) the RPKM values (Reads Per Kilobase of exon per Million fragments mapped) for that gene were above 5 RPKM in the cranial neural crest; (2) difference in expression levels was significant according to statistical analysis at FDR of 0.05 (3) the gene had at least 2-fold upregulation in the cranial neural crest. The table with expression levels of the genes enriched in the cranial neural crest (Database S1) contains values for samples that were processed as replicates in Cufflinks/Cuffdiff. Two genes that were previously identified as cranial-specific (*Ets1* (*18*) and *Brn3c*) failed statistical analysis due to

improper genomic annotation; they were included in the *in situ* hybridization screen and subsequent perturbation analysis.

Cloning of cranial genes and *in situ* hybridization

Cranial genes identified in the transcriptome analysis were cloned using the TOPO TA Cloning Kit Dual Promoter (Invitrogen). cDNA was synthesized with SuperScript® III Reverse Transcriptase (Invitrogen), from RNA obtained from dissected cranial neural folds obtained from HH8-HH10 chicken embryos. Whole mount *in situ* hybridization was performed as described (*19*) with modifications including more extensive washes and a CHAPS-based hybridization buffer. Double fluorescent *in situ* hybridization was performed using the Tyramide TSA system from Perking Elmer (TSA Plus Cyanine 5 & Fluorescein, NEL754001KT), as previously described (*20*).

Fate-mapping

The fate map of neural crest progenitors was generated at stages HH8- (3 somites) by injection of a single spot of CellTracker *CM-DiI* on the dorsal surface of the neural plate border of individual embryos (*21*). The embryos were incubated overnight, until they reached stage HH 12, when the embryos were fixed and analyzed for the position of the labeled cells. The fate map was compiled by marking the coordinates of each individual injection spot onto the image of a representative embryo, and color-coding the spots according to their fate at stages HH12 (cranial or vagal/trunk neural crest). To compare the fate map with the expression of the cranial-specific regulators, we generated a spatial average of the *Dmbx1* expression domain. We registered the expression pattern of this gene from several HH8- embryos and created an overlap of expression domains onto the fate map by using a coordinate grid (Fig. 2D).

Perturbation experiments

In all perturbation experiments, we employed bilateral injections, where the two sides of the embryos were transfected with different reagents (*11*). The left side (control) was injected with biotin-labeled control morpholinos or control expression vectors. The right side (experimental) was injected with FITC-labelled targeted morpholinos or expression vectors. All embryos were screened prior to further analysis; embryos with weak or incomplete electroporation, or with morphological abnormalities were discarded. Visualization of biotin-labelled control morpholino was performed by incubating morphants with 1ng/ul Streptavidin conjugated to Alexa Fluor 647 (Molecular Probes, S32357) in PBS Triton (0.3%) for 2 hours, followed by 3 washes of 5 minutes in PBST. The following morpholinos were used: Control (ATGGCCTCGGAGCTGGAGAGCCTCA) Dmbx1 (CGTTCACCCCATAGTGCTGCATGGC), Lhx5 (AGCCCGCACAATGCACCATCATCAC), Sox8 (TCCTCGGTCATGTTGAGCATTTGG), Tfap2b (CAACCAGTTTCCAGAGCATGATGGC) and Ets1 (GCTTCAGGTCCACCGCCGCCTTCAT). Efficiency of morpholinos was tested by fusing the UTRs and the coding sequence of the first 10 amino acids of target genes to GFP; electroporation of these constructs with the targeted morpholinos resulted in absence of GFP expression (Fig. S2). The Brn3c dominant negative construct was

designed according to a previously published expression vector used for Brn2 loss of -function (*22*). Effects on downstream genes where scored by comparison between targeted (right) and control (left) neural folds of the same embryo; we surveyed gene expression of putative downstream targets by *in situ* hybridization and qPCR. In the qPCR analysis, all possible interactions between the 5 factors and Ets1 where surveyed. Target for the in situ hybridization analysis were chosen based on onset of gene expression shown on Fig. 2E. The sample size for each knockdown experiment was determined according to what is deemed appropriate according to the standards of the field. No randomization or blinding was performed in the described assays.

Quantitative analysis of gene expression

For qPCR analysis following knockdown of cranial specific transcription factors, embryos were electroporated bilaterally with morpholinos or dominant negative constructs (described above), and the expression profile of the targeted neural fold was compared to the control side (Fig. 3I). The two neural folds of morphant embryos were microdissected at stages HH8-9 and lysed for cDNA synthesis. Samples were prepared for RT-qPCR analysis using the TaqMan Cells-to-CT Kit from Ambion, following the manufacture's instructions. Real-time qPCR analysis was performed on an ABI PRISM Applied BioSystems 7000 Sequence Detection System using Power SYBR® Green Master Mix (Thermo Fisher Scientific). We designed primers for *Brn3c*, *Lhx5*, *Dmbx1*, *Sox8*, *Tfap2b*, *Ets1* and *Hprt1* with the Primer3Plus program (http://www.bioinformatics.nl/cgi-bin/primer3plus/primer3plus.cgi); real-time PCR efficiencies were determined for all sets of designed primers. Expression levels of target gene were normalized to the expression of *Hprt1*, and relative changes in mRNA expression between control and loss of function neural folds were determined through the $2^{-\Delta\Delta Ct}$ method. Abundance of each cranial specific gene in a targeted neural fold is presented relative to the expression levels of the same gene in the control neural fold of the same embryo (Fig. 3I). Significant changes in expression levels were determined by unpaired Student's t-test ($P < 0.05$).

Chromatin immunoprecipitation (ChIP)

To identify direct interactions between cranial specific transcription factors and downstream targets we employed biotin-ChIP (*23*). Brn3c, Lhx5, Dmbx1, Sox8, Tfap2b were fused with an AVI tag and cloned in pCI:H2B-RFP. Embryos were electroporated at gastrula stage (HH5) with each of these constructs and a vector driving nuclear expression of the E. coli enzyme BirA (pCI:NLS-BirA-Cer), and incubated until stage HH8-9. For each experiment, 20 embryos were dissected in Ringer's solution and chromatin prepared from dorsal neural folds was immunoprecipitated as described (*23, 24*) using the MyOne™ Streptavidin T1 Dynabeads. Mock controls were transfected with pCI:NLS-BirA-Cer only. Enrichment for a specific DNA sequence was calculated using the comparative CT method. Since the cis-regulatory apparatus the target genes have not all been characterized, we designed primers to target the promotor sequences of these genes with the rationale that active transcription factor-bound enhancers loop at the chromatin level to interact with their respective promoters; thus, crosslinked pulldowns will carry the relevant enhancer and promoter DNA sequences (*24*). For additional controls we employed primers targeting intergenic negative control regions (NCR). All

primers were designed with the Primer3Plus program. In Fig. 3K the results are presented as fold enrichment of control ChIP experiment done with IGG Dynabeads; for each experiment the same chromatin was split between Streptavidin T1 Dynabeads and the control IGG Dynabeads. The results on Fig. S4 are presented as percent of total input used in each immunoprecipitation.

Enhancer reprogramming experiments

For targeted expression of cranial factors in the trunk neural crest, the coding sequences of *Brn3c*, *Lhx5*, *Dmbx1* were cloned in pCI:H2B-RFP(*8*). M. Barembaum generously provided the *Sox8* and *Tfap2b* expression constructs, which were cloned in the same vector. The *Ets1* expression vector was available from previous studies (*8*). *In ovo* electroporation was performed according to the guidelines described by Nakamura and Funahashi (*25*). In the reprogramming experiments, separate vectors encoding each transcription factor were co-electroporated. The trunk neural tubes of HH10-11 embryos were injected with combinations of expression vectors and electroporated with platinum electrodes (five 50ms pulses of 20.5V, with an interval of 100ms between pulses). After electroporation, embryos were incubated until stage HH14 and analyzed for ectopic activity of cranial enhancer Sox10E2 in the trunk neural crest. Other enhancers tested in these experiments were Sox10E1 (*8*), NC2 (*9*) and Ets1ECR3 (*26*). Expression levels of cranial genes in the reprogrammed trunk neural crest were assayed by qPCR. As targets, we tested genes that are involved in chondrocytic differentiation (*Runx2* and *Alx1*) and are enriched in the cranial neural crest (*10*). The expression levels of reprogrammed cells were compared to wild type cranial neural crest (HH10, obtained with the cranial Sox10E2 enhancer) and wild type trunk neural crest (HH14, obtained with the trunk Sox10E1 enhancer). Pure populations of wild type and reprogrammed neural crest were obtained through FACS; cDNA was synthesized with the Power SYBR® Green Cells-to-CT™ Kit (Ambion 4402953). The bar graphs on Fig. 4F-G represent the average normalized levels of *Alx1*, *Runx2*, *Dbx2* and *Hes6* gene expression obtained from three biological replicates of the experiment (three distinct FACS sorting sessions).

Enhancer reprogramming experiments

To test the chondrocytic potential of wild type and reprogrammed trunk neural crest, we employed Roslin Green GFP Eggs purchased from Clemson University. Mock transfected or reprogrammed trunk neural folds were microdissected from HH11 GFP+ donor embryos and grafted into the heads of HH9 wild type hosts (Fig. S7). The chimeras were incubated until embryonic day (E) 7, by which time endogenous cartilage cells have differentiated, and fixed for histological analysis (see below). We tested the chondrocytic potential of mock transfected trunk neural crest, which was electroporated with pCI:H2B-RFP (n=0/5), and reprogrammed trunk neural crest, which had been transfected with expression vectors driving expression of *Sox8*, *Tfap2b* and *Ets1* (n=4/7).

Sectioning and immunohistochemistry

For histological analysis, grafted embryos were washed in 5% and 15% sucrose and incubated in 17% gelatin for 3 hours at 37°C. Embedded embryos were frozen with liquid nitrogen and sectioned at 10-15 μm with a Micron cryostat. For immunostaining we used the protocol previously described (*21*). Slides were de-gelatinized, washed in TBS with

0.3% Triton supplemented with 0.1% DMSO and blocked for 2 hours in the same solution supplemented with 10% donkey serum. The following antibodies were used: anti-GFP antibody produced in rabbit (1:300, Thermo A6455), anti-Collagen type IX produced in mouse (1:1, DSHB 2C2) anti-Collagen type II produced in mouse (1:1, DSHB II-II6B3). Secondary antibodies used included donkey anti-rabbit IGG, or donkey anti-mouse IGM, conjugated with Alexa Fluor 488/555/594/647 (1:2000, Molecular probes). For imaging, slides were stained with DAPI and mounted with PermaFluor Mounting Medium (Thermo 434990).

Fig. S1

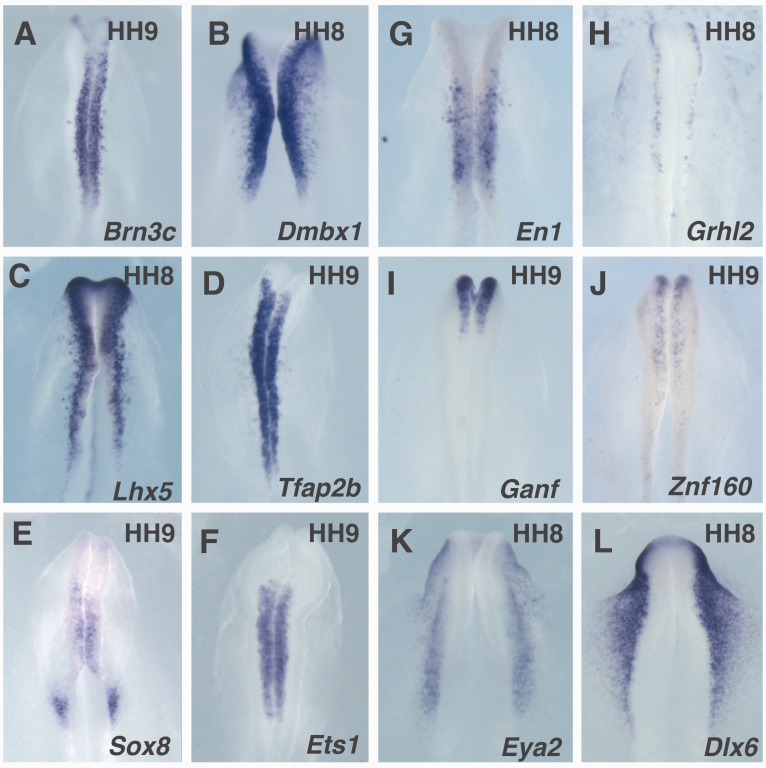

Figure S1. *In situ* hybridization screen of genes enriched in the cranial neural crest. Analysis of expression patterns confirms enrichment of cranial-specific transcriptional regulators in the cranial neural crest. These included genes expressed by the whole cranial neural crest population (**A-F**), as well as transcripts present in subsets of cells (**G-L**). All pictures show dorsal views of the cephalic regions of chicken embryos after chromogenic *in situ* hybridization.

Fig. S2

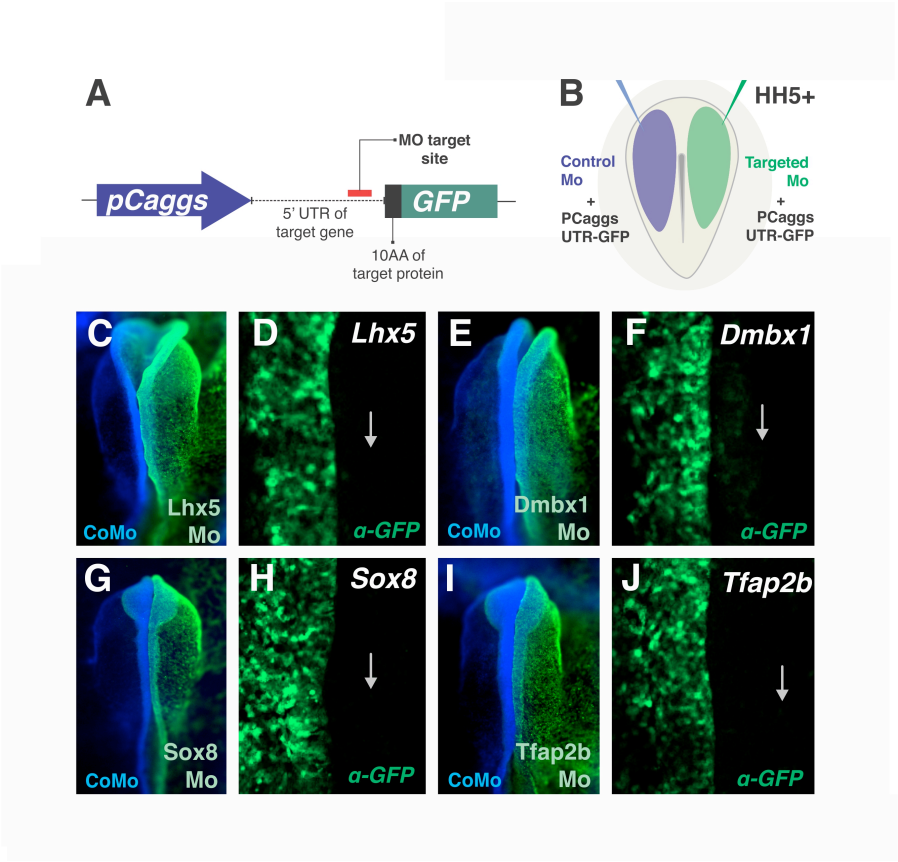

Figure S2. Validation of morpholino knockdown efficiency. (**A**) Diagram of expression constructs for testing morpholino efficiency with *in vivo* translation blocking assays. The UTR and 10 first amino acids of each target genes, which contain the morpholino target site, were fused to eGFP. This cassette was cloned downstream of a pCaggs constitutive promoter. (**B**) Bilateral electroporation of control (blue) and targeted (green) morpholinos in different sides of the embryo. Both sides were also co-transfected with the corresponding expression constructs. (**C**) Whole-mount dorsal view of embryo after Lhx5 morpholino (Mo) and control morpholino (CoMo) were transfected to the right and left side of each embryo, respectively. (**D**) Dorsal view of the embryo pictured in (C), showing loss of GFP expression caused by the LhxMO on the right side of the embryo (n=8/8). (**E-J**) Validation of Dmbx1 (n=8/8), Sox9 (n=9/9) and Tfap2b (n=8/8) morpholinos. AA: aminoacids.

Fig. S3

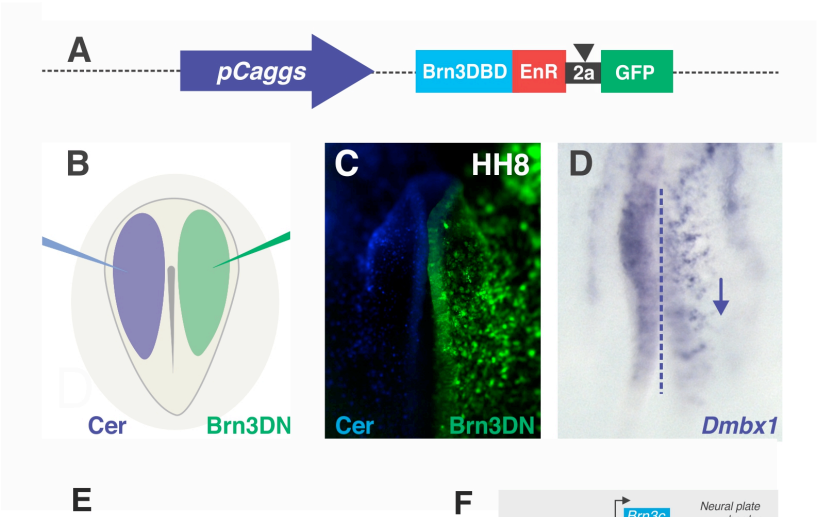

E

KD	Target	Phenotype* WT	Mild	Strong	N
Brn3c	*Lhx5*	100	00.0	00.0	*23*
	Dmbx1	14.3	86.7	00.0	*21*
Lhx5	*Sox8*	00.0	22.8	77.8	*18*
	Tfap2b	04.5	18.2	77.3	*22*
Dmbx1	*Sox8*	76.5	23.5	00.0	*17*
	Tfap2b	05.0	10.0	85.0	*20*
Sox8	*Tfap2b*	100	00.0	00.0	*12*
	Ets1	88.9	11.1	0.00	*18*
Tfap2b	*Sox8*	91.7	08.3	00.0	*12*
	Ets1	00.0	20.0	80.0	*20*

*Percent of total embryos

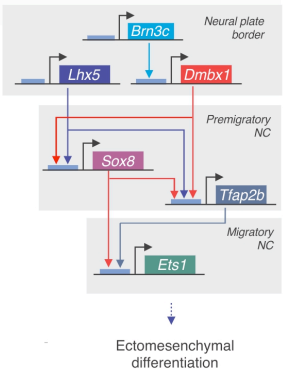

Figure S3. Supporting data for loss of function analysis. (**A**) Brn3c dominant negative construct. The Brn3c DNA binding domain (DBD) was fused with to an Engrailed repressor domain (EnR), and cloned downstream of a pCaggs constitutive promoter. An eGFP reporter linked to the fusion protein with a 2a self-cleaving peptide was added to the vector to monitor transfection efficiency. (**B**) Diagram of bilateral electroporation of stage HH4 embryos. (**C**) Whole-mount dorsal view of embryo after the dominant negative (Brn3DN) and a control construct (pCaggs-Cerulean) were transfected to the right and left side of each embryo, respectively. (**D**) The same embryos as (C), after *in situ* hybridization for Dmbx1, with downward blue arrows indicating disruption of gene expression on the experimental side (n=10/12). (**E**) Table summarizing loss-of-function experiments, including the number embryos displaying mild (partial loss), strong (complete loss) or no effect on putative downstream targets after knockdown of each regulator. (**F**) Gene regulatory interactions revealed by loss of function and qPCR analysis. The diagram is based on the data presented on Figure 3I; interactions likely to be indirect were omitted.

Fig. S4

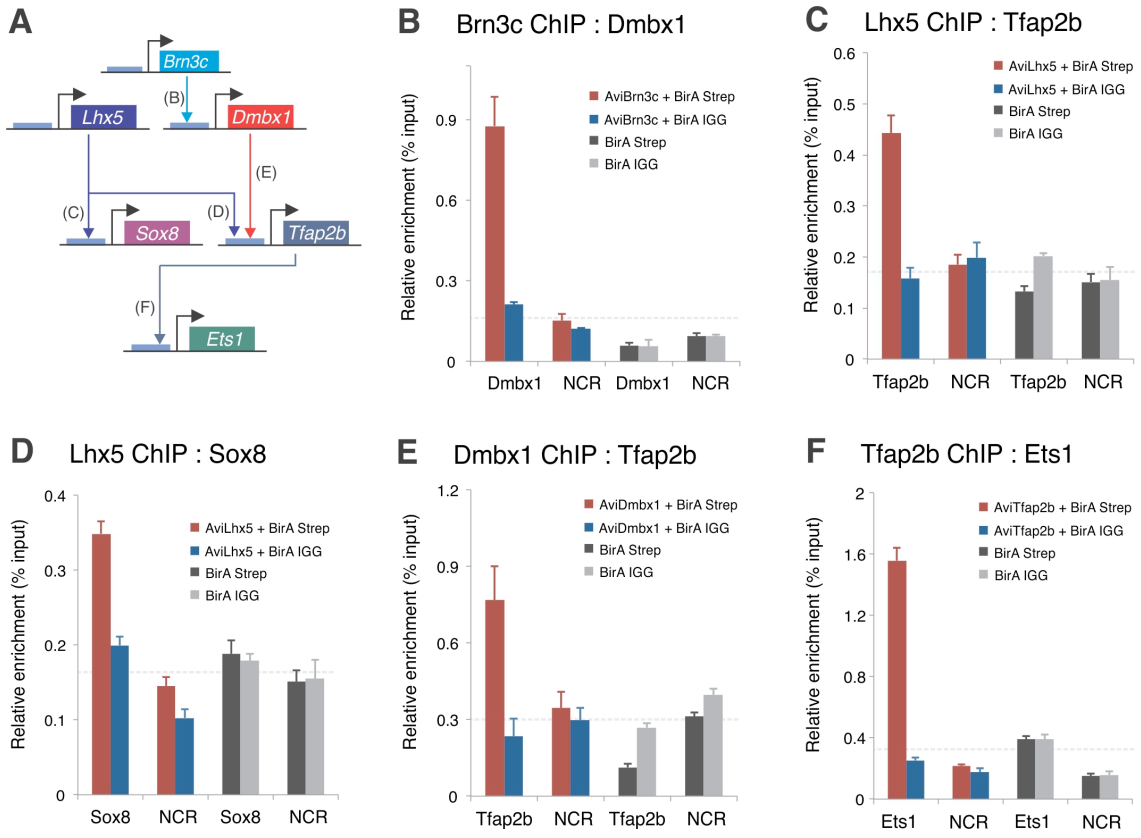

Figure S4. Chromatin immunoprecipitation (biotin-ChIP) analysis reveals transcription factor - promoter interactions in the cranial specific neural crest circuit. (**A**) Diagram showing the transcription factor (TF) promoter interactions tested via biotin ChIP. (**B-F**) ChIP assay performed in dissected dorsal neural folds of stage HH9 embryos co-electroporated with expression constructs encoding Avi-tagged TFs and the *E. coli* BirA enzyme. IP of the transcription factors protein with Streptavidin Dynabeads, followed by site specific qPCR with primer pairs designed to amplify the promoter region of the putative downstream target revealed significant enrichment of the target region in the TF pull-down when compared to IGG controls. No enrichment was observed for negative control regions (NCR) chosen in intergenic regions, or when the experiment was conducted on embryos transfected with BirA only. Enrichment of amplicons is expressed as a percent of the total input chromatin used in the IP assay. Error bars represent SD.

Fig. S5

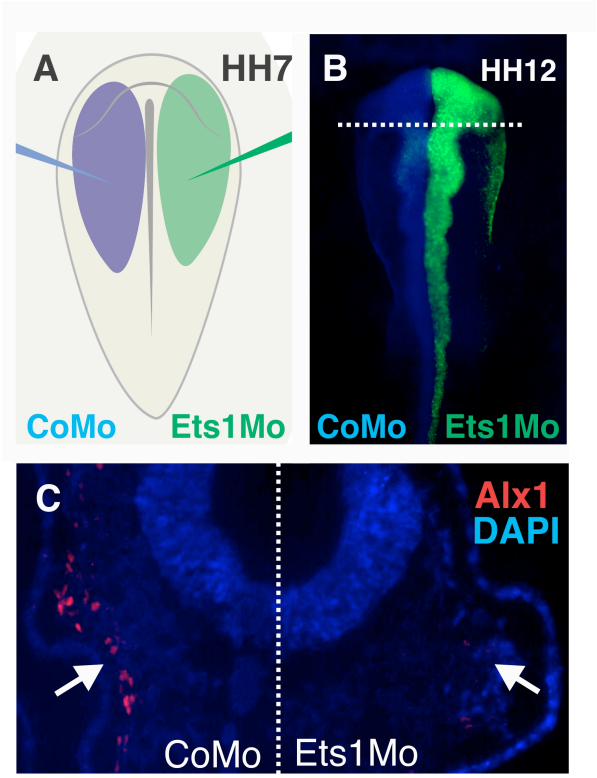

Figure S5. *Ets1* is required for expression of *Alx1* in the late migratory neural crest. (**A**) Diagram of bilateral electroporation of stage HH7 embryos. (**B**) Whole-mount dorsal view of a HH12 embryo after the *Ets1* morpholino (Ets1Mo) and control morpholino (CoMo) were transfected to the right and left side of each embryo, respectively. (**C**) Transverse section through the midbrain region of the embryo depicted in (B). The right side of the embryo, which was electroporated with the *Ets1* morpholino, displays loss of *Alx1* expression (red) in the late migratory neural crest population (n=7/8), as assayed by immunohistochemistry with an anti-Alx1 antibody.

Fig. S6

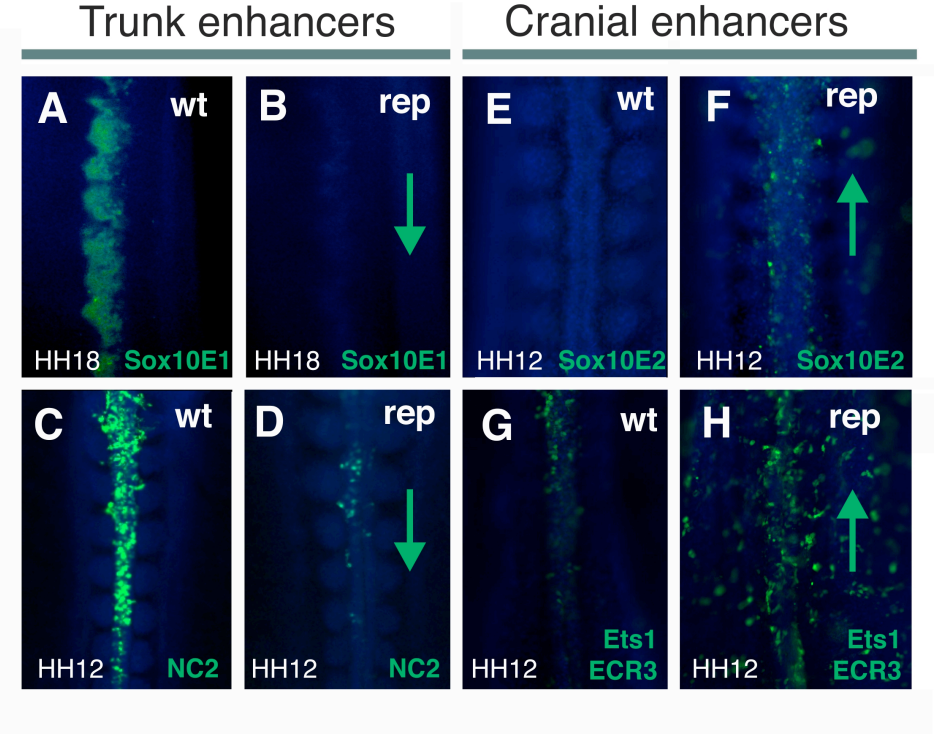

Figure S6. Effects of trunk neural crest reprogramming on trunk- and cranial-specific enhancers. Reprogramming with cranial-specific regulators impacts activity of neural crest trunk- and cranial-specific enhancers. (**A**) The Sox10E1 enhancer is active in trunk neural crest populations in wild type (wt) conditions. (**B**) Reprogramming of the trunk neural crest with cranial factors results in loss of Sox10E1 activity. (**C and D**) The trunk FoxD3 enhancer NC2 is also repressed in reprogrammed trunk neural crest cells. (**E-H**) Cranial-specific enhancers Sox10E2 and Ets1ECR3 are ectopically activated in trunk neural crest cells following reprogramming. wt: wild type. rep: Reprogrammed.

Fig. S7

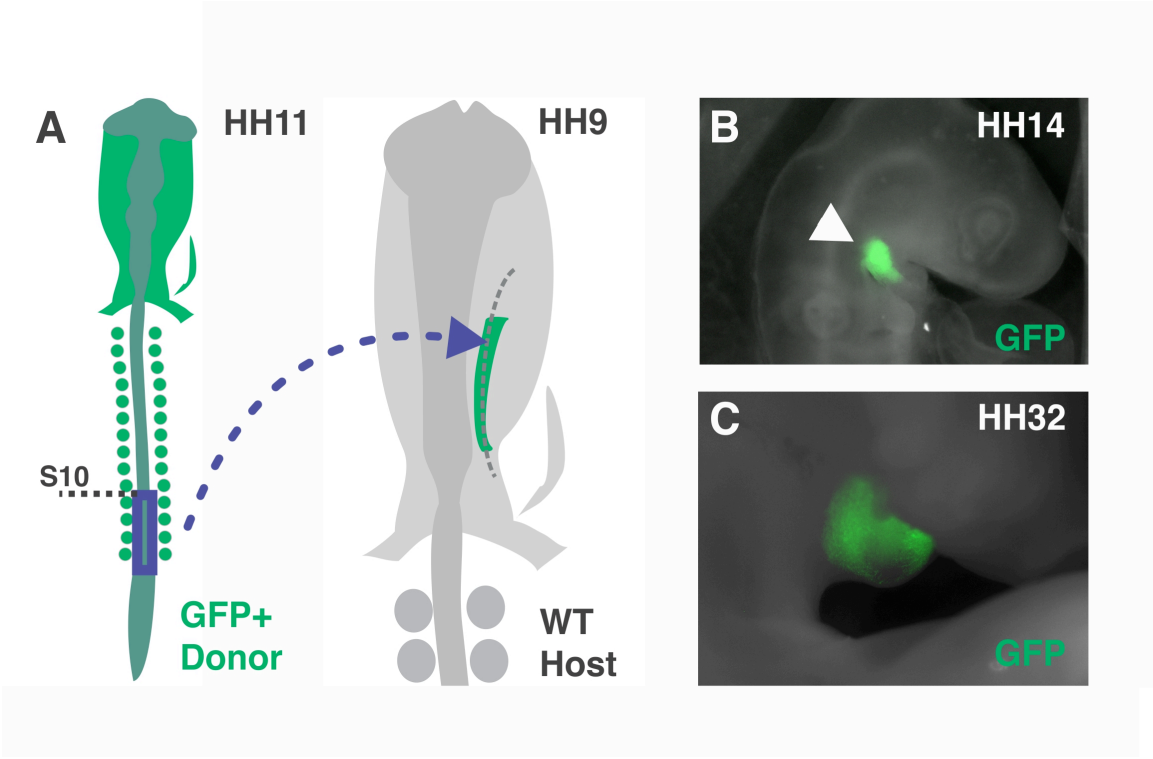

Figure S7. Testing neural crest potential with chimeric embryos. (**A**) Diagram of neural crest grafts utilizing GFP+ transgenic embryos. Trunk neural folds were dissected from HH11 GFP+ embryos donor embryos from regions posterior to the 10th somite (S10). The cells were transplanted to the cranial regions of HH9 wild type embryos. Each graft was placed adjacent to the hindbrain. (**B and C**) Control embryos photographed after grafting at stages HH14 and HH32, showing GFP+ neural crest cells invading the jaw.

Database S1. Transcripts enriched in cranial neural crest cells identified by comparative RNA-seq analysis of neural crest subpopulations. This dataset has been deposited in NCBI's Gene Expression Omnibus under accession number GSE75125. (https://www.ncbi.nlm.nih.gov/geo/query/acc.cgi?acc=GSE75125)

REFERENCES

1. N. Le Douarin, *The Neural Crest* (Cambridge Univ. Press, 1982).

2. M. Simões-Costa, M. E. Bronner, Insights into neural crest development and evolution from genomic analysis. *Genome Res.* **23**, 1069–1080 (2013). Medline doi:10.1101/gr.157586.113

3. T. Uesaka, M. Nagashimada, H. Enomoto, Neuronal differentiation in Schwann cell lineage underlies postnatal neurogenesis in the enteric nervous system. *J. Neurosci.* **35**, 9879–9888 (2015). Medline doi:10.1523/JNEUROSCI.1239-15.2015

4. V. Dyachuk, A. Furlan, M. K. Shahidi, M. Giovenco, N. Kaukua, C. Konstantinidou, V. Pachnis, F. Memic, U. Marklund, T. Müller, C. Birchmeier, K. Fried, P. Ernfors, I. Adameyko, Parasympathetic neurons originate from nerve-associated peripheral glial progenitors. *Science* **345**, 82–87 (2014). Medline doi:10.1126/science.1253281

5. C. S. Le Lièvre, N. M. Le Douarin, Mesenchymal derivatives of the neural crest: Analysis of chimaeric quail and chick embryos. *J. Embryol. Exp. Morphol.* **34**, 125–154 (1975). Medline

6. C. S. Le Lievre, G. G. Schweizer, C. M. Ziller, N. M. Le Douarin, Restrictions of developmental capabilities in neural crest cell derivatives as tested by in vivo transplantation experiments. *Dev. Biol.* **77**, 362–378 (1980). Medline doi:10.1016/0012-1606(80)90481-9

7. P. Y. Lwigale, G. W. Conrad, M. Bronner-Fraser, Graded potential of neural crest to form cornea, sensory neurons and cartilage along the rostrocaudal axis. *Development* **131**, 1979–1991 (2004). Medline doi:10.1242/dev.01106

8. P. Betancur, M. Bronner-Fraser, T. Sauka-Spengler, Genomic code for Sox10 activation reveals a key regulatory enhancer for cranial neural crest. *Proc. Natl. Acad. Sci. U.S.A.* **107**, 3570–3575 (2010). Medline doi:10.1073/pnas.0906596107

9. M. S. Simões-Costa, S. J. McKeown, J. Tan-Cabugao, T. Sauka-Spengler, M. E. Bronner, Dynamic and differential regulation of stem cell factor FoxD3 in the neural crest is encrypted in the genome. *PLOS Genet.* **8**, e1003142 (2012). Medline doi:10.1371/journal.pgen.1003142

10. M. Simões-Costa, J. Tan-Cabugao, I. Antoshechkin, T. Sauka-Spengler, M. E. Bronner, Transcriptome analysis reveals novel players in the cranial neural crest gene regulatory network. *Genome Res.* **24**, 281–290 (2014). Medline doi:10.1101/gr.161182.113

11. M. Simões-Costa, M. Stone, M. E. Bronner, Axud1 integrates Wnt signaling and transcriptional inputs to drive neural crest formation. *Dev. Cell* **34**, 544–554 (2015). Medline doi:10.1016/j.devcel.2015.06.024

12. M. Simões-Costa, M. E. Bronner, Establishing neural crest identity: A gene regulatory recipe. *Development* **142**, 242–257 (2015). Medline doi:10.1242/dev.105445

13. S. A. Green, M. Simoes-Costa, M. E. Bronner, Evolution of vertebrates as viewed from the crest. *Nature* **520**, 474–482 (2015). Medline doi:10.1038/nature14436

14. T. Sauka-Spengler, M. Barembaum, Gain- and loss-of-function approaches in the chick embryo. *Methods Cell Biol.* **87**, 237–256 (2008). Medline doi:10.1016/S0091-679X(08)00212-4

15. S. C. Chapman, J. Collignon, G. C. Schoenwolf, A. Lumsden, Improved method for chick whole-embryo culture using a filter paper carrier. *Dev. Dyn.* **220**, 284–289 (2001). Medline doi:10.1002/1097-0177(20010301)220:3<284::AID-DVDY1102>3.0.CO;2-5

16. C. Trapnell, L. Pachter, S. L. Salzberg, TopHat: Discovering splice junctions with RNA-Seq. *Bioinformatics* **25**, 1105–1111 (2009). Medline doi:10.1093/bioinformatics/btp120

17. C. Trapnell, B. A. Williams, G. Pertea, A. Mortazavi, G. Kwan, M. J. van Baren, S. L. Salzberg, B. J. Wold, L. Pachter, Transcript assembly and quantification by RNA-Seq reveals unannotated transcripts and isoform switching during cell differentiation. *Nat. Biotechnol.* **28**, 511–515 (2010). Medline doi:10.1038/nbt.1621

18. E. Théveneau, J. L. Duband, M. Altabef, Ets-1 confers cranial features on neural crest delamination. *PLOS ONE* **2**, e1142 (2007). Medline doi:10.1371/journal.pone.0001142

19. D. G. Wilkinson, *In Situ Hybridization: A Practical Approach* (IRL Press at Oxford Univ. Press, 1992).

20. N. Denkers, P. García-Villalba, C. K. Rodesch, K. R. Nielson, T. J. Mauch, FISHing for chick genes: Triple-label whole-mount fluorescence in situ hybridization detects simultaneous and overlapping gene expression in avian embryos. *Dev. Dyn.* **229**, 651–657 (2004). Medline doi:10.1002/dvdy.20005

21. A. M. Ezin, S. E. Fraser, M. Bronner-Fraser, Fate map and morphogenesis of presumptive neural crest and dorsal neural tube. *Dev. Biol.* **330**, 221–236 (2009). Medline doi:10.1016/j.ydbio.2009.03.018

22. D. S. Kim, T. Matsuda, C. L. Cepko, A core paired-type and POU homeodomain-containing transcription factor program drives retinal bipolar cell gene expression. *J. Neurosci.* **28**, 7748–7764 (2008). Medline doi:10.1523/JNEUROSCI.0397-08.2008

23. J. Kim, A. B. Cantor, S. H. Orkin, J. Wang, Use of in vivo biotinylation to study protein-protein and protein-DNA interactions in mouse embryonic stem cells. *Nat. Protoc.* **4**, 506–517 (2009). Medline doi:10.1038/nprot.2009.23

24. K. E. Kolodziej, F. Pourfarzad, E. de Boer, S. Krpic, F. Grosveld, J. Strouboulis, Optimal use of tandem biotin and V5 tags in ChIP assays. *BMC Mol. Biol.* **10**, 6 (2009). Medline doi:10.1186/1471-2199-10-6

25. H. Nakamura, J. Funahashi, Introduction of DNA into chick embryos by in ovo electroporation. *Methods* **24**, 43–48 (2001). Medline doi:10.1006/meth.2001.1155

26. M. Barembaum, M. E. Bronner, Identification and dissection of a key enhancer mediating cranial neural crest specific expression of transcription factor, Ets-1. *Dev. Biol.* **382**, 567–575 (2013). Medline doi:10.1016/j.ydbio.2013.08.009